Circular Polarized Patch Antenna for 5.8 GHz Dedicated Short-Range Communication

Daniel Megnet #1, Heinz Mathis #2

Institute for Communication Systems, HSR University of Applied Sciences
Oberseestrasse 10, 8640 Rapperswil, Switzerland
[1] daniel.megnet@hsr.ch
[2] heinz.mathis@hsr.ch

***Abstract*— A circular polarized patch antenna for the 5.8 GHz dedicated short-range communication (DSRC) band is proposed. This frequency band includes road transport and traffic telematics (RTTT) applications, which impose severe cost and size limitations on microwave RTTT devices.**

The patch antenna is based on low-cost, but lossy, FR-4 material. It consists of a rectangular radiator patch, which is fed by a single feed point, Because of the size limitations, detuning and power loss caused by the device case are taken into consideration. A design method for the antenna, which is based on EM simulations and equations, is given.

The proposed 5.8 GHz patch antenna shows low sensitivity to manufacturing tolerances. EM simulation results are compared to theoretical considerations and measurements results. Special attention has been given to the radiation pattern and cross-polarization ratio, which both are regulated by RTTT standards.

I. Introduction

Wireless applications constantly move up the frequency scale. Whereas the 2.4 GHz band gets rather crowded, people try to resort to frequencies at and above 5 GHz. Between 5 and 6 GHz, very diverse applications can be found such as WLAN, dedicated short-range communication (DSRC), and ISM applications. One of the more prominent types of antennas used in this band is the patch antenna.

The proposed antenna has been optimized for dedicated short-range communication (DSRC) in the 5.8 GHz frequency band. This frequency band is used for road transport and traffic telematics (RTTT) and an RF link usually consists of multiple, mobile on-board units (OBU) and a single, fixed roadside unit (RSU).

For RTTT applications to be efficient, a high percentage of vehicles must be equipped with an OBU. Thus, these devices must be manufactured in high quantities at low costs. In order to keep costs low, the OBU is usually a battery powered, passive RF device, which is activated by a received carrier signal. Bidirectional communication is realized by changing the reflexion coefficient of the antenna feed network. Thus, received signals are reradiated to the RSU with a modulated phase.

II. Antenna Design Requirements

The RTTT preconditions have a large impact on the antenna design. The antenna gain pattern must be reasonably wide in order to get a long enough communication time while passing a RSU with high speed. On the other hand, the transmit and the receive antenna being the same, the antenna gain and efficiency counts twice, once for the reception of the unmodulated carrier and once for the retransmission of the carrier. The European standard EN 12253 [1] regulates the minimum and maximum conversion gain for a reflected signals, as well as the cross-polarization ratio (CPR) for the OBU in order to ensure reliable communication. However, EN 12253 does not regulate the antenna pattern itself. Thus, the minimal antenna gain primarily depends on other system parameters. Left-hand circular polarized (LHCP) signals are used for the communication link between RSU and OBU. The total bandwidth of an RTTT application according to EN 12253 is 20 MHz (0.36 %)

The OBU, being a low-cost device, prohibits the use of special microwave substrates for its antenna. Thus, the antenna design is limited to inexpensive but lossy FR-4 PCB material.

III. Circular Polarized Patch Antenna

The proposed antenna consists of an FR-4 substrate, which carries the GND layer and the feed circuit, and a thin, rectangular metal radiator patch. The patch is separated from the substrate by an air layer. This stacked dielectric design reduces the dielectric losses without causing additional costs and results in a mixed substrate that has a low permittivity, which increases the bandwidth of the antenna. Although bandwidth is not a major concern for RTTT applications, it nonetheless relaxes manufacturing tolerances. However, a strong interferer in a nearby band can activate the OBU, which results in reduced battery life if the bandwidth is too high.

The patch of the proposed antenna is not attached to the feed substrate, but to the plastic case. Fig. 1 and Fig. 2 shows the construction of the proposed antenna.

A. Circular Polarization

The proposed antenna is a circular polarized, rectangular patch. For this type of antenna, it is easy to get circular polarization by exciting two orthogonal modes with slightly different resonance frequencies. These two modes are modeled with two second-order parallel-resonant circuits defined by

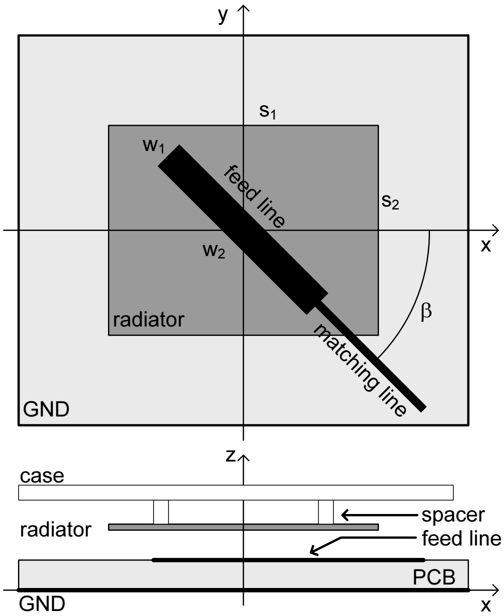

Fig. 1. Antenna design parameter of 5.8 GHz LHCP patch antenna.

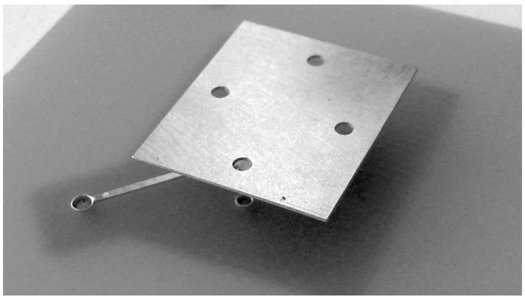

Fig. 2. 5.8 GHz microstrip antenna on FR-4 substrate without case.

their resonance frequencies ω_{0i} and Q-factors Q_i. The normalized impedance of an excited mode i is [2]

$$Z_i(s) = \frac{\frac{R}{Q_i \omega_{0i}} s}{1 + \frac{1}{Q_i \omega_{0i}} s + \frac{1}{\omega_{0i}^2} s^2}, \quad s = j\omega,\ R = 1, \tag{1}$$

The angle between the electric field vectors of both modes is given by the geometry of the antenna and is assumed to be 90° for the rectangular patch antenna at hand. The phase difference between both modes is

$$\alpha(\omega) = \phi_2 - \phi_1 = \arg\left(Z_2(\omega)\right) - \arg\left(Z_1(\omega)\right). \tag{2}$$

In order to calculate the polarization ratio (PR) of a rectangular patch antenna, a simple model of the antenna consisting of two resonance modes is assumed. The first mode has an electric field E_1 parallel to the unit vector $\mathbf{e}_x$, and the second mode has an electric field E_2 parallel to the unit vector $\mathbf{e}_y$. All field quantities are shown in Fig. 3. Both modes are excited with the same signal but with different magnitudes a and b and different phases ϕ_1 and ϕ_2. Thus, the resulting electric field vector is

$$E = E_1 + E_2 \sim a \cdot \cos(\omega t)\mathbf{e}_x + b \cdot \cos(\omega t + \alpha)\mathbf{e}_y. \tag{3}$$

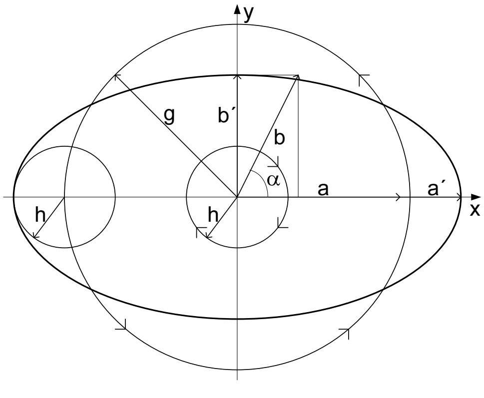

Fig. 3. Axial ratio and cross-polarization calculation.

A common measure for the quality of the achieved circular polarization is the axial ratio. It is defined as

$$R_{\text{axial}} \triangleq \frac{E_{\max}}{E_{\min}} = \frac{a'}{b'}. \tag{4}$$

Alternatively, the CPR is often used to describe the polarization quality. An elliptically polarized signal consists of a left-hand circular polarized (LHCP) wave and a right-hand circular polarized (RHCP) wave with magnitude g and h, respectively. Thus the resulting electric field vector is

$$E = E_1 + E_2 \sim g \cdot e^{+j\omega t} + h \cdot e^{-j\omega t}, \tag{5}$$

and the CPR is

$$R_{\text{cross}} \triangleq \frac{g}{h}, \qquad g > h. \tag{6}$$

Phase and amplitude errors of the excited modes can be normalized to orthogonal modes according to Fig. 3 with

$$\begin{aligned} a' &= g + h = a + b\cos\alpha \\ b' &= g - h = b\sin\alpha. \end{aligned} \tag{7}$$

Thus, the CPR defined by (6) is

$$R_{\text{cross}} = \frac{a' + b'}{a' - b'} = \frac{a + b(\cos\alpha + \sin\alpha)}{a + b(\cos\alpha - \sin\alpha)}. \tag{8}$$

A phase difference deviation does not per se result in a degraded PR but can be corrected by changing the magnitude ratio a/b. The magnitude ratio that compensates for a given phase difference α in order to produce a certain CPR can be calculated by rearranging (8),

$$R_{\text{mag}} = \frac{a}{b} = \frac{R_{\text{cross}} + 1}{R_{\text{cross}} - 1} \cdot \sin(\alpha) - \cos(\alpha). \tag{9}$$

B. Antenna Patch Design

The phase of a single radiation mode depends on its Q-factor and on its resonance frequency. An estimate for the resonance frequency of a microstrip antenna is [3]

$$f_{0i} \approx \frac{c_0}{2\sqrt{\varepsilon_{\text{r,eff}}}(s_i + 2\Delta L)}. \tag{10}$$

TABLE I

CALCULATED AND SIMULATED PROPERTIES OF THE PROPOSED ANTENNA.

mode	size	calculated			simulated	
i	s_i/mm	ΔL/mm	f_{0i}/GHz	Q_i	f_{0i}/GHz	Q_i
1	17.63	1.72	5.758	-	5.673	70.7
2	14.98	1.72	6.566	-	5.850	85.2

The length extension ΔL, which is caused by fringing fields has been estimated with equations given in [4]. The mean relative permittivity of the stacked dielectric is

$$\varepsilon_{\text{r,tot}} = (h_{\text{air}} + h_{\text{pcb}}) \cdot \frac{\varepsilon_{\text{r,air}}\varepsilon_{\text{r,PCB}}}{h_{\text{PCB}}\varepsilon_{\text{r,air}} + h_{\text{air}}\varepsilon_{\text{r,PCB}}}. \quad (11)$$

The effective permittivity $\varepsilon_{\text{r,eff}}$ can be estimated if the permittivity of the dielectric is known. However, the well known equation [3]

$$\varepsilon_{\text{r,eff}} = \frac{\varepsilon_{\text{r}} + 1}{2} + \frac{\varepsilon_{\text{r}} - 1}{2}\left(1 + 12\frac{h}{w}\right)^{-1/2} \quad (12)$$

is based on a homogenous dielectric, thus, a small error must be allowed for. The antenna prototypes are built with an 1.4 mm air layer and an 1.5 mm PCB layer. For the FR-4 based PCB, $\varepsilon_{\text{r,PCB}} = 4.6$ is assumed, resulting in $\varepsilon_{\text{r,tot}} = 1.68$. The Q-factor in (1) is more difficult to calculate. The Eigen-mode solver of Ansoft HFSS has been used to analyze the Q-factors as well as the resonance frequencies of this antenna including the OBU case and a 50 Ω load at the end of the feed line.

Previous EM simulations already showed that a radiator size of $s_1 = 17.63$ mm and $s_2 = 14.98$ mm results in a good CPR at 5.8 GHz. Thus, these dimensions are used for all further considerations. The resonance frequencies of these two modes according to (10) along with the Eigen-mode analysis results are given in Table I. As expected, the resonance frequencies given by HFSS are different because the electric field distribution on which [4] is based is different from the distribution in the stacked dielectrics used to build the antenna. Further error sources are detuning caused by the case cover and dielectric losses, which both are accounted for in the simulation.

The PR calculation result is shown in Fig. 4. The PR at 5.8 GHz is poor if a constant power distribution between both modes according to (8) is used. However, the frequency-dependent return loss $\Gamma_i(f)$ of each mode given by (1) also causes a non-constant power distribution

$$R_{\text{mag}}(f) = \frac{a}{b} = \sqrt{\frac{1 - |\Gamma_2(f)|^2}{1 - |\Gamma_1(f)|^2}}. \quad (13)$$

The frequency-dependent power distribution, which is shown in Fig. 4, too, causes a CPR maxima at 5.8 GHz.

C. Antenna Feed Design and Matching

A proximity feed technique has been used to excite the radiator patch because it allows for excitation of the patch without galvanic connection, thus, manufacturing is simplified. However, proximity-fed antennas need a good aligning between feed and radiator. Holes in the radiator patch are used to mount the radiator (see Fig. 2). Furthermore, a proximity feed has an inherent higher impedance bandwidth and more degrees of freedom for the matching of the antenna than a galvanic connection [3].

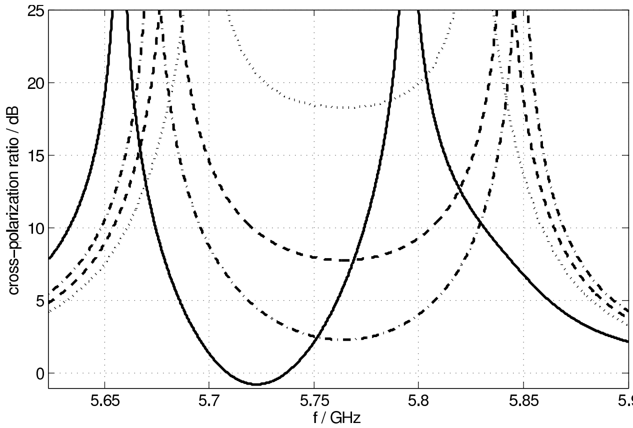

Fig. 4. Calculated PR depending on frequency and power distribution between both modes. Dashed: $a/b = 0$ dB, dash-dotted: $a/b = -2$ dB, dotted: $a/b = +2$ dB, solid: a/b depends on Γ_i.

The feed consists of a rectangular feed line with $w_1 = 1.8$ mm and $w_2 = 12.8$ mm. This feed line is rotated by $\beta = 45°$ in order to excite both modes of the patch. w_1, w_2, β and are the main means for tuning the antenna. However, these parameters influence the polarization and resonance frequencies, because they change the return loss of the resonance modes. The antenna has been matched to 50 Ω with an additional 0.62 mm wide microstrip matching line.

IV. RESULTS

A. Simulation Results

The proposed antenna, including a simplified plastic case, has been simulated with Ansoft HFSS. Fig. 5 shows a plot of the simulated CPR at boresight as well as the return loss. The best CPR and optimum matching are not at the same frequency. The maximum simulated CPR is about 16 dB at 5.80 GHz. Polarization is limited mainly by higher-order modes, which are neglected in the simplified model used to calculate the CPR [5], [6].

Most of the dielectric power loss is caused by the PCB. Simulations showed that about 8.9 % of the power is dissipated in the FR-4 PCB. Only about 0.15 % is dissipated in the plastic case cover. Thus, the case only detunes the antenna but does not cause significant power loss.

B. Measurement Results

Two prototypes of the proposed antenna have been built; one with a spacing of 3.5mm between the case and the FR-4 PCB and one with a reduced spacing of 2.4 mm, as this is the most critical manufacturing parameter. Helical antennas with a CPR of 20 dB have been used to measure the patch antenna parameters.

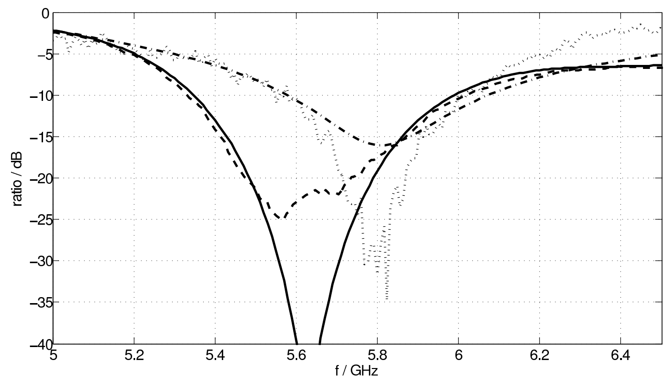

Fig. 5. Return-loss and polarization of an antenna prototype with spacing of 3.5 mm between case and PCB. Solid: simulated $|S_{11}|$, dashed: measured $|S_{11}|$, dash-dotted: simulated CPR, dotted: measured CPR.

Fig. 5 shows the return-loss of the antenna prototype as well as the CPR. Both measurements correspond well with the simulation results. However, the high return loss of the simulated antenna could not be reached. An impedance bandwidth of 650 MHz (11%) and a polarization bandwidth of about 400 MHz (7%) has been achieved, which is well above the requirements. According to the simulations, the antenna is expected to have a CPR of -16 dB. However, if measured with the reference antennas, this can result in a measured CPR between -12 dB and -25 dB, depending on the relative orientation of the antennas [7]. Fig. 5 shows that the measured CPR can be up to -30 dB, which indicates a real CPR of at least -16 dB. Fig. 6 shows the RHCP and LHCP antenna pattern of the two prototypes. The orientation and generic shape of the OBU case used is shown, too. The radiator location is indicated by a thin line. A CPR of about -13 dB was obtained.

According to [1], the CPR must be more than 10 dB at boresight and more than 6 dB at the -3 dB points in the antenna pattern. These specifications are achieved by both antenna prototypes in spite of the non-symmetrical antenna pattern. This distortion is caused by the OBU case, which has a bulge at 270°. Only -3 dB antenna gain relative to the boresight gain is allowed at 35° in practical RTTT applications. This parameter is critical because of the strong influence of the case.

V. Conclusion

A low-cost, FR-4 based 5.8 GHz patch antenna has been proposed. The antenna uses a proximity feed technique in order to get a large bandwidth and thus small sensitivity to manufacturing tolerances. Dielectric losses are kept low due to the layered dielectric used. A simple design method for the antenna, which bases on the transmission line model for microstrip antennas and EM-simulations, is given. Theoretical considerations and simulation results as well as measurement results match very well. An 11% impedance bandwidth and 7% polarization bandwidth have been achieved, thus, the proposed type of antenna can also be used for broad band applications. The measured antenna parameters conform to the requirements of road transport and traffic telematics devices.

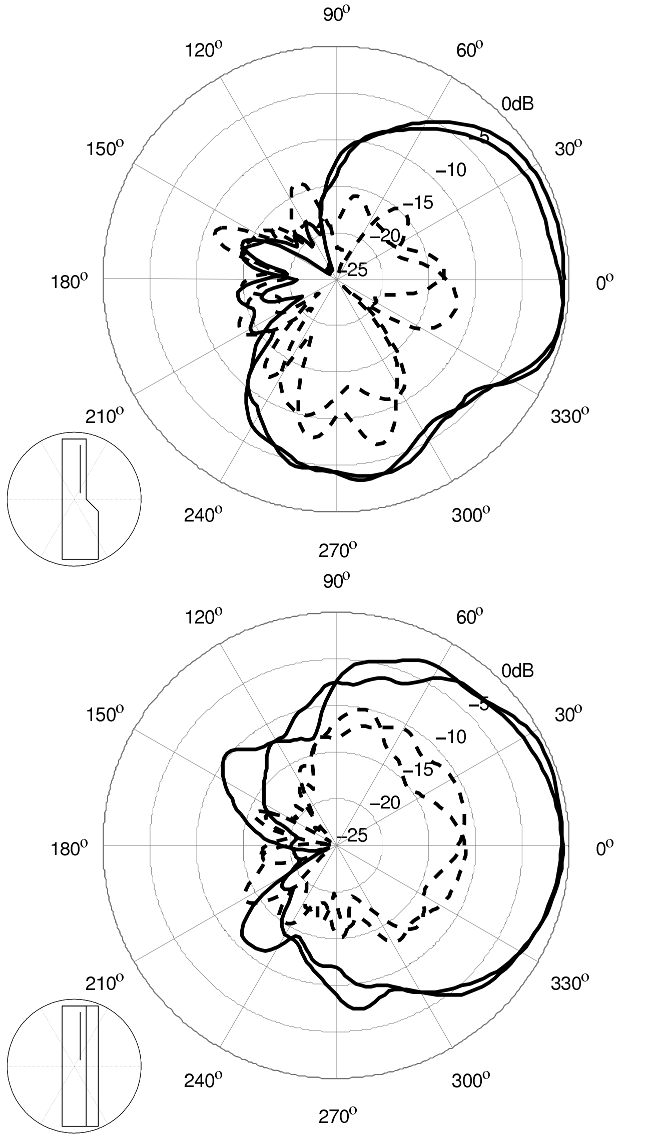

Fig. 6. Vertical (top) and horizontal (bottom) antenna pattern of two antenna prototypes with different spacing at 5.8 GHz. Solid: LHCP, dashed: RHCP.

References

[1] *EN 12253, Road transport and traffic telematics - Dedicated short-range communication - Physical layer using microwave at 5,8 GHz*, CEN European Standard, 2004.

[2] D. K. Misra, *Radio-Frequency and Microwave Communication Circuits: Analysis and Design*, 1st ed. John Wiley & Sons, 2001.

[3] C. A. Balanis, *Antenna Theory Analysis and Design*, 2nd ed. John Wiley & Sons, 1997.

[4] E. O. Hammerstad, "Equations for microstrip circuit design," in *Proc. 5th Europ. Microwave Conf.*, Hamburg, Germany, 1975, pp. 268–272.

[5] J. Huang, "A technique for an array to generate circular polarization with linearly polarized elements," in *Antennas and Propagation, IEEE Transactions on*, vol. 34, no. 9, 1986, pp. 1113–1124.

[6] T. Chiba, Y. Suzuki, and N. Miyano, "Suppression of higher modes and cross polarized component for microstrip antennas," in *IEEE Antennas and Propagation Society International Symposium*, vol. 20, 1982, pp. 285–288.

[7] "IEEE standard test procedures for antennas," *ANSI/IEEE Std 149-1979*, pp. –, Dec 1979.